P92-A2

NASA CR- 177872

1N-7473

GERNERATION OF AVAILABLE POTENTIAL ENERGY

AND THE ENERGY CYCLE DURING

THE GLOBAL WEATHER EXPERIMENT

Second year final report on contract number NAS5-27745

David A. Salstein

Richard D. Rosen

Atmospheric and Environmental Research, Inc.

840 Memorial Drive

Cambridge, Massachusetts 02139

April 1986

1. INTRODUCTION

During the first year of our contract, we pursued two major themes. The first of these involved examining the impacts of satellite-based data and the forecast model used by the Goddard Laboratory for Atmospheres (GLA) on general circulation statistics. This work has resulted in a manuscript which we submitted for publication in the current contract year. (Salstein et al., 1986).

For the other major topic, we examined the diabatic heating fields produced by GLA for one month during the FGGE First Special Observing Period. As part of that effort we studied the three-dimensional distribution of the four component heating fields, namely those due to shortwave radiation, Q_{SW}, longwave radiation, Q_{LW}, sensible heating, Q_S, and latent heating, Q_L. These components were calculated as part of the GLA analysis/forecast system (Kalnay et al., 1983; Baker, 1983), and archived every quarter day; from these archives cross products with temperature were computed to enable the direct calculation of certain terms of the large-scale atmospheric energy cycle, namely those involving the generation of available potential energy (APE).

These generation terms had been computed in the past primarily by a residual approach; this approach was necessary largely because accurate estimates of the distribution of diabatic heating based on a global data set were not available prior to FGGE. Thus, the inclusion of diabatic heating in the GLA model-produced fields has allowed a direct calculation of the individual generation terms. Furthermore, the decision to archive the diabatic heating components separately has enabled us to study the role of the various processes that drive the energy cycle of the atmosphere.

2. DIABATIC HEATING CROSS-SECTIONS

Fields of total diabatic heating and components for our study period (January 6 - February 4, 1979) were presented as part of our first year final report (Salstein and Rosen, 1985). Here we have taken the zonal averages of these fields and display them in a latitude-pressure cross-section for the diabatic heating components (Figure 1) and for total diabatic heating (Figure 2). These figures represent the mean heating rate in degrees per day that occurs above the earth's surface. Evident is the importance in the tropics of latent heating, which peaks near the 400 mb level. Both latent and sensible heating are especially strong just above the surface layer in the northern

hemisphere mid-latitudes. The influence of longwave radiation is to provide
cooling (negative heating) everywhere. Above the lowest layer, maximum long-
wave cooling occurs nearest the equator, and at the surface the maximum cool-
ing tends to take place in the tropics of each hemisphere, though some 10-20°
latitude away from the equator. Shortwave radiational heating is positive
everywhere south of the northern high latitudes of the winter polar night.

The latitudinal distribution of these component and total heating fields,
vertically averaged between the 1000 and 100 mb levels, is shown in Figures 3
and 4. Prominent here is the equatorial peak in the latent heating processes,
which extends through the southern hemisphere tropics. The other processes
have profiles that are somewhat smoother, so the shape of the total, particu-
larly in low latitudes, tends to be dominated by that of latent heating. As
was evident from the cross-sections, latent and sensible heating have peaks
near 40° N and longwave radiation provides its maximum cooling in the tropics.
The maximum total cooling, though, due to the sum of the diabatic processes,
occurs in areas nearest the north pole.

3. GENERATION OF AVAILABLE POTENTIAL ENERGY

As stated earlier, the diabatic heating fields have been used to compute
the terms in the atmospheric energy cycle related to the generation, G, of
available potential energy. We have concentrated during this year on the
approximate Lorenz formulation, and thus calculated the G terms, in the frame-
work of Peixoto and Oort (1974). In this formulation G is separated into that
of the zonal mean form of APE, $G(P_M)$ [in Figures written as G(Z)], and that of
the eddy form of APE, $G(P_E)$ [in the Figures G(E)]. The traditional Lorenz
approach involves the calculation of the G terms from a static stability
factor γ, which is horizontally averaged over the globe or hemisphere, and
from the temperature and various heating fields:

$$G(P_M) = \iint \gamma(p)[\overline{T}]''[\overline{Q}]'' dm$$

$$G(P_E) = G(P_{TE}) + G(P_{SE}) = \iint \gamma(p)([\overline{T'Q'}] + [\overline{T^*\overline{Q}^*}]) dm$$

Here an overbar denotes temporal mean over the month-long study period, a
prime departure from it, a brackets zonal mean, and an asterisk departure
therefrom. T denotes temperature and Q stands for a heating rate. The double

prime is equivalent to departure from a hemispheric or global mean:

$$[\ ]'' = [\ ] - \int [\ ] \cos \phi d\phi \quad ,$$

ϕ is latitude and dm an element of mass. As indicated above, we have considered the generation of available potential energy by both transient eddies (TE) and standing eddies (SE). The static stability factor is a function of pressure alone in the Lorenz (1967) formulation and is equivalent to:

$$\gamma = (\frac{1000}{p})^\kappa \ (\frac{\kappa}{p}) \quad (\frac{\partial [\tilde{\theta}]}{\partial p})^{-1}$$

where $\kappa = 2/7$, and $[\tilde{\theta}]$ is the global (or hemispheric) mean potential temperature, θ, on a pressure surface, and θ is computed:
$[\tilde{\theta}] = [\overline{T}](1000/p)^\kappa$, where pressure, p, is given in millibars.

Cross-sections in the latitude-pressure plane of the integrands of $G(P_M)$ from the four heating components and total are given, respectively, in Figures 5 and 6. The correlations between the mean temperature fields and the heating fields, modified by the static stability, are responsible for the integrand fields. We see, for example, positive numbers in the integrand for latent heating in the tropics, where both heating and temperature are higher than their hemispheric means. Additionally the integrand is positive as well in high latitudes, where heating and temperature are both lower than hemispheric means. In the integrand for longwave radiational heating (cooling), the sign is negative almost thoughout, due to the negative correlation of temperature with its heating. (The atmosphere radiates more heat away at higher temperatures.) Shortwave radiation provides lesser impact to the integrand except at high latitudes in the northern hemisphere, where an absence of radiation is equivalent to lower than mean values. Finally the impact of sensible heating is significant only at the lowest levels. The total integrand appears to have the character largely of the latent heating components.

Vertical integrals of these integrand cross-sections for the components and totals (Figures 7 and 8) show the positive nature of the integrands in the tropics and the high contribution from the northern hemisphere high latitudes, though the total area at these high latitudes is small.

The integrands of the generation of eddy available potential energy including the transient and standing forms, are given in Figures 9 and 10 for

3

the heating components and total heating, respectively. The integrands are in general of smaller magnitude than those of $G(P_M)$; however sensible heating causes a relatively large generation of P_E at low levels in northern hemisphere mid-latitudes.

Figures 11-13 shows the contributions to the total integrands of the generation of transient and standing eddies forms of available potential energy, at three levels in the atmosphere: 925 mb, 850 mb, and 500mb. The same types of contributions are given for the latent heating components, as an example, in Figures 14-16. One interesting result is shown in Figure 16 for the contribution to the generation of transient eddy available potential energy at 500 mb by latent heating. Especially apparent in this figure is the difference in character between the baroclinically driven mid-latitudes (positive generation) and the convectively-driven tropics (negative generation). Despite the substantial negative areas in this figure, the overall contribution by latent heating to the sum of the transient and standing eddy forms of APE through the depth of the atmosphere is positive, as indicated in Table 1.

We have also evaluated the generation terms in the more exact Boer (1975) framework, formulas for which are as follows:

$$G(P_M) = \iint [\overline{N}][\overline{Q}] \ dm$$

$$G(P_E) = \iint \gamma(\phi,p) \ ([\overline{T'Q'}] + [\overline{T^*\overline{Q}^*}]) \ dm$$

Here $[\overline{N}]$ is an "efficiency factor" (see Lorenz, 1967) and the stability factor γ is based upon latitude as well as pressure.

While this form is not equivalent to the fully exact equations (e.g., Dutton and Johnson, 1967), it preserves the form of these equations in pressure coordinates as far as possible while permitting the separation of G into zonal mean and eddy forms. The Boer results for the generation terms are also given in Table 1. There it can be seen that the relative strengths of the generation of APE by the various components using this approach are similar to those based on the Lorenz formulation.

4. DECOMPOSITION OF GENERATION TERMS INTO WAVENUMBER SPACE

The generation of APE by the heating components occurs on all spatial

scales, and a breakdown into zonal wavenumber of the standing eddy form has been performed by means of the formulation of Saltzman (1957):

$$G_n = \int\int \gamma(\phi,p) \ \Phi_{Q,T,n}(\phi,p) \ dm$$

where $\quad \Phi_{Q,T,n} = \{F_Q(n) \ F_T(-n) + F_Q(-n) \ F_T(n)\}$

and F is the Fourier Transform:

$$F_X(n) = \frac{1}{2\pi} \int_0^{2\pi} X(\lambda) \ e^{-in\lambda} d\lambda.$$

The results for the four components and total diabatic heating are given in Figures 18 and 19. We see the importance of the first few wavenumbers and, in particular, that of wavenumber 2, in which latent heat dominates the total. The strength of wavenumber 2 may have partly originated from the continent-ocean contrast dominant at this scale. The latitudinal distribution of the generation of the first six wavenumber components, as well as those for total standing eddy generation, is given in Figure 20. There we see the especially prominent peaks near 20°S and between 50° and 70° N.

5. DIURNAL VARIABILITY OF HEATING CROSS-SECTIONS

The diabatic heating component fields for the month were segregated initially by synoptic hour. Pictures of the monthly mean fields for four synoptic hours, 00, 06, 12, 18 GMT at two pressure levels were given by Salstein and Rosen (1985). Zonal averages of the vertical means of these fields were calculated, and the variation of the mean heating at the four hours is displayed here. The departures of the fields from a 24-hour mean are given for the four heating components in Figure 21. The most variability occurs in sensible heating, followed by latent heating. The variability of both longwave and shortwave radiational heating is small. In the sensible heating figure, the strong peak at 15° N at 12 GMT, for example, appears to be due to the midday heating from the West African land mass at that synoptic time, while the 06 GMT peak near 20° S originates from the Australian region. The variability displayed in these figures indicates the overall importance of including terms on a more than once per day basis in studies involving diabatic heating.

6. CONCLUDING REMARKS

We have analyzed the various components of diabatic heating through the depth of the atmosphere for one northern hemisphere winter month during the FGGE First Special Observing Period, and we used these fields to ascertain the role of the heating components in the atmospheric energy cycle. Our future plans involve the examination of the heating fields and the related energy generation terms from a period during the northern hemisphere summer, and so the seasonal variability in atmospheric heating will be able to be studied.

It should be stressed, finally, that the heating rates studied here have been produced by the physics package of the GLA analysis/forecast system, and so are model dependent. Further work comparing these heating fields with other estimates, such as from thermodynamic methods (e.g., Johnson et al., 1985), is being planned.

7. REFERENCES

Baker, W. E., 1983: Objective analysis and assimilation of observational data from FGGE. Mon. Wea. Rev., 111, 328-342.

Boer, G. J., 1975: Zonal and eddy forms of the available potential energy equations in pressure coordinates. Tellus, 27, 433-442.

Dutton, J. A. and D. R. Johnson, 1967: The theory of available potential energy and a variational approach to atmospheric energetics. Advances in Geophysics, 12, Academic Press, N. Y., pp. 333-436.

Johnson, D. R., R. D. Townsend and M.-Y. Wei, 1985: The thermally coupled response of the planetary scale circulation to the global distibution of heat sources and sinks. Tellus, 37A, 106-125.

Kalnay, E., R. Balgovind, W. Chao, D. Edelmann, J. Pfaendtner, L. Takacs, and K. Takano, 1983: Documentation of the GLAS fourth order general circulation model. NASA Technical Memorandum 86064. [NTIS N8424028]

Lorenz, E. N., 1967: The Nature and Theory of the General Circulation of the Atmosphere. World Meteorological Organization, Geneva, 161 pp.

Peixoto, J. P. and A. H, Oort, 1974: The annual distribution of atmospheric energy on a planetary scale. J. Geophys. Res., 79, 2149-2159.

Salstein, D. A. and R. D. Rosen, 1985: Generation of available potential energy and the energy cycle during the global weather experiment. First year final report on contract number NAS5-27745.

Salstein, D. A., R. D. Rosen, W. E. Baker and E. Kalnay, 1986: Impact of satellite-based data on FGGE general circulation statistics. Manuscript submitted to Q. J. Roy. Meteor. Soc.

Saltzman, B., 1957: Equations governing the energetics of the larger scales of atmospheric turbulence in the domain of wave number, J. Meteor., 14, 289-299.

GENERATION OF AVAILABLE POTENTIAL ENERGY

Global average in watts m^{-2}

	Shortwave	Longwave	Sensible	Latent		Total Diabatic
$G(P_M)$						
Lorenz	1.39	−2.55	0.19	3.41		2.44
Boer	1.55	−4.22	1.67	4.43		3.43
$G(P_E)$						
Lorenz	0.11	−0.31	−0.07	0.56		0.29
Boer	0.08	−0.16	−0.03	0.32		0.22

Table 1

SHORTWAVE HEATING

SENSIBLE HEATING

LONGWAVE HEATING

LATENT HEATING
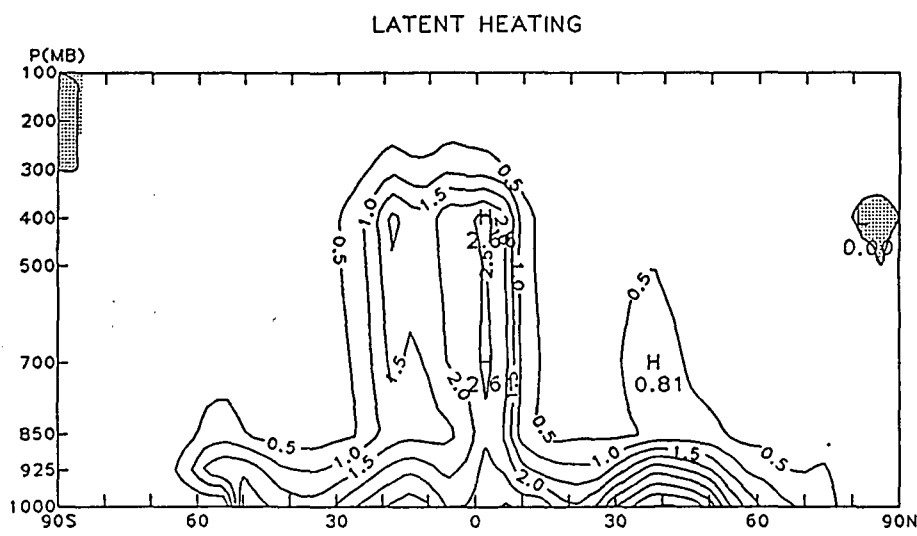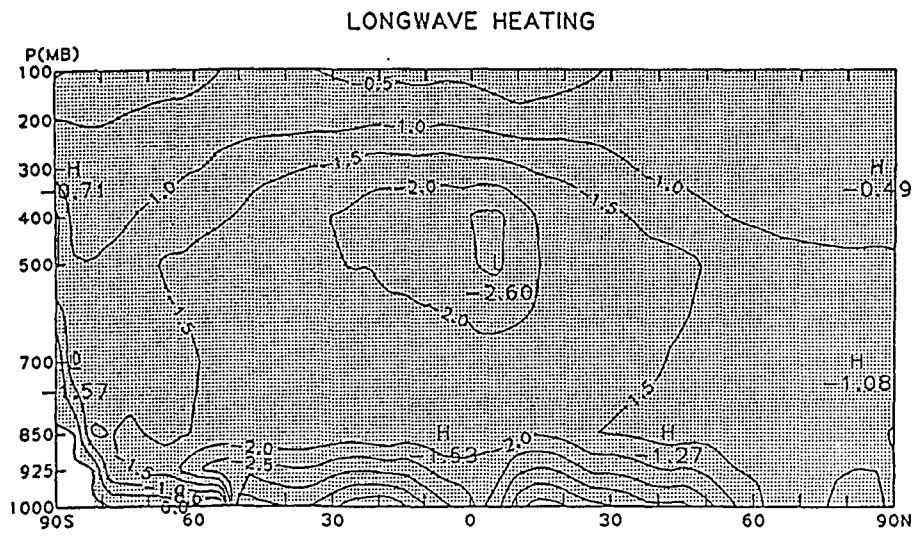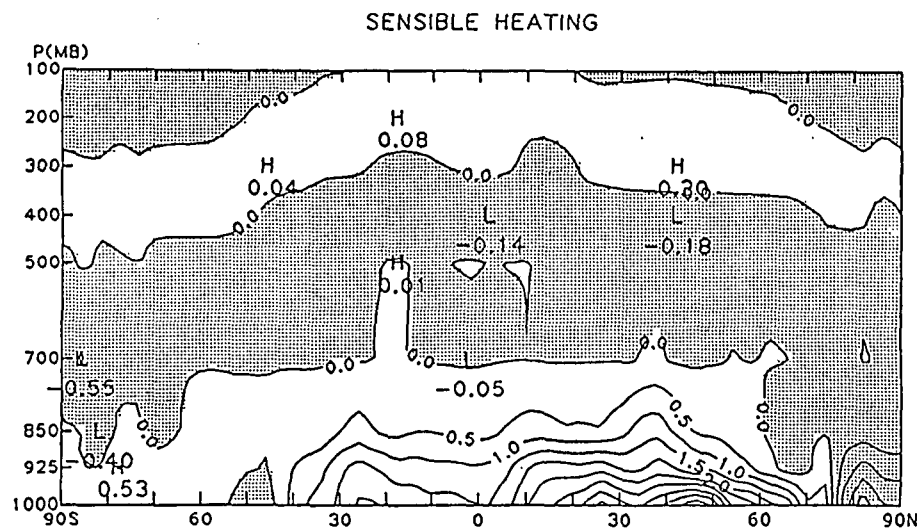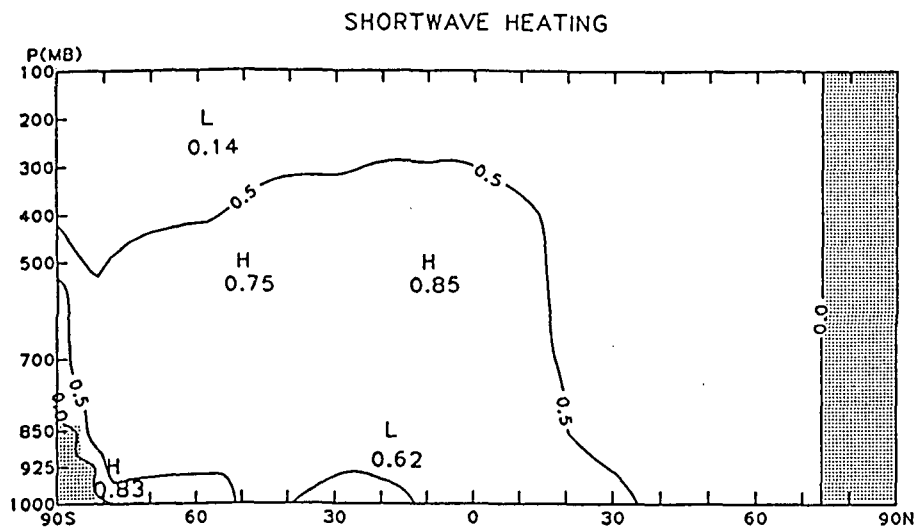
Fig. 1   Zonal mean heating, in °C day^{-1}, by each of four components for January 6 –
February 4, 1979.
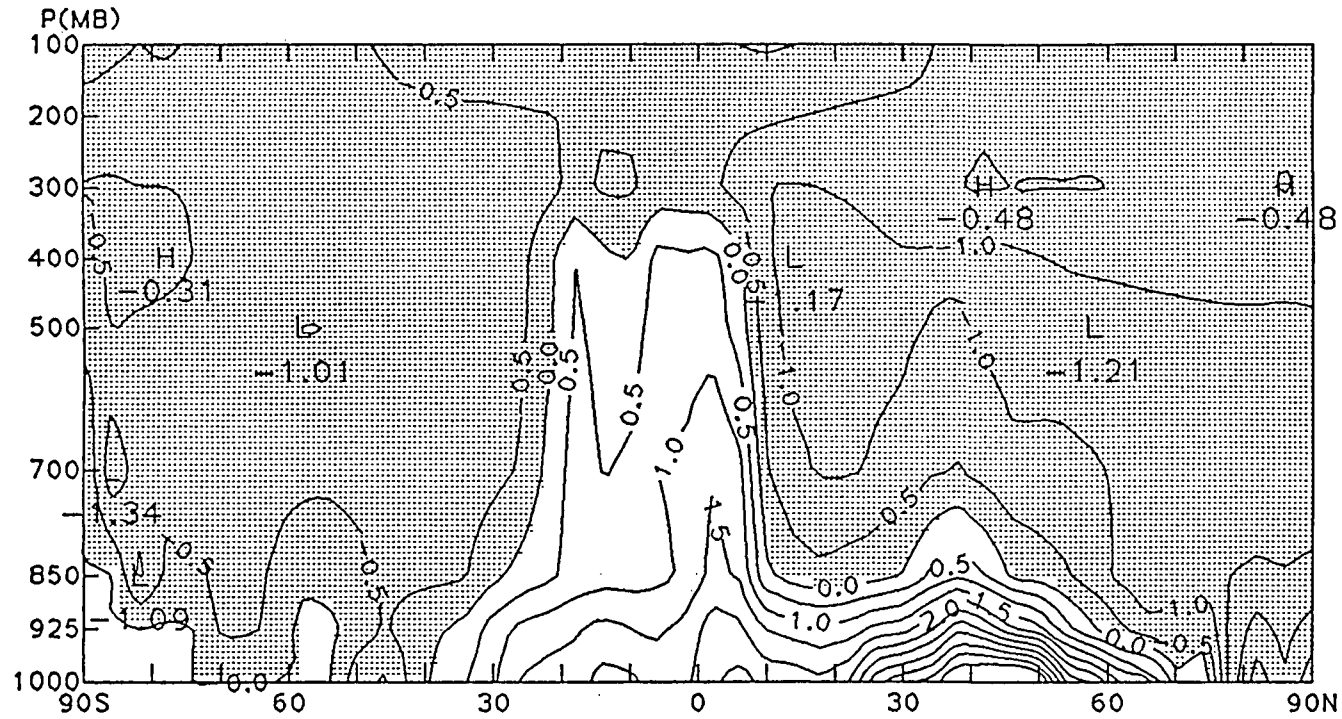
DIABATIC HEATING

Fig. 2   Zonal mean total diabatic heating, in °C day^{-1}, for January 6 – February 4, 1979.

AVERAGE HEATING — COMPONENTS   °C DAY^{-1}

LATENT

SHORTWAVE

SENSIBLE

LONGWAVE

LATITUDE
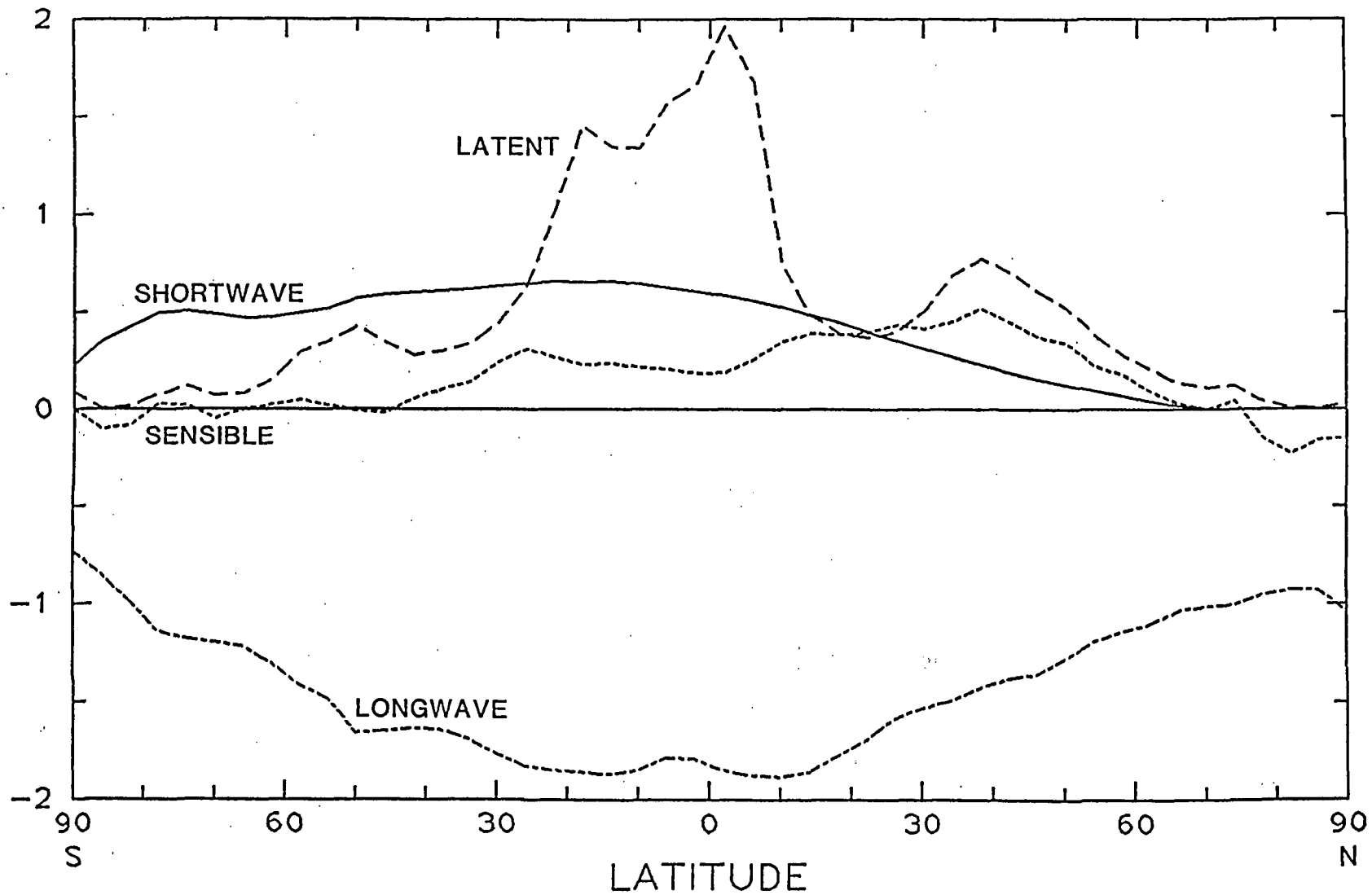
Fig. 3   Vertically averaged zonal mean heating, in °C day^{-1}, by four components for January 6 – February 4, 1979.

AVERAGE HEATING – TOTAL   °C DAY⁻¹
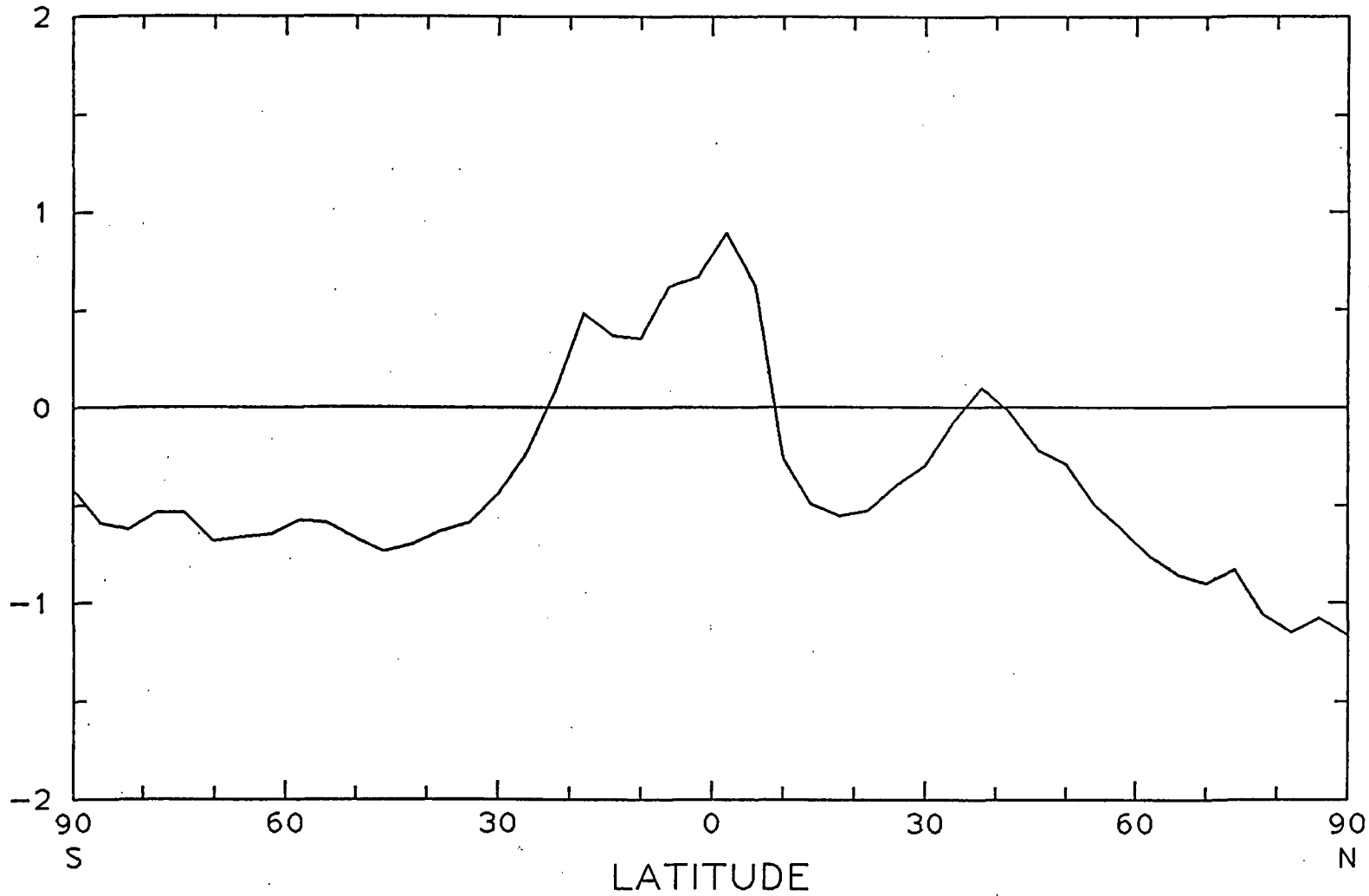
Fig. 4   Vertically averaged mean total diabatic heating, in °C day⁻¹, for January 6 – February 4, 1979.

INTEGRAND OF G(Z) – SHORTWAVE HEATING

INTEGRAND OF G(Z) – SENSIBLE HEATING

INTEGRAND OF G(Z) – LONGWAVE HEATING

INTEGRAND OF G(Z) – LATENT HEATING
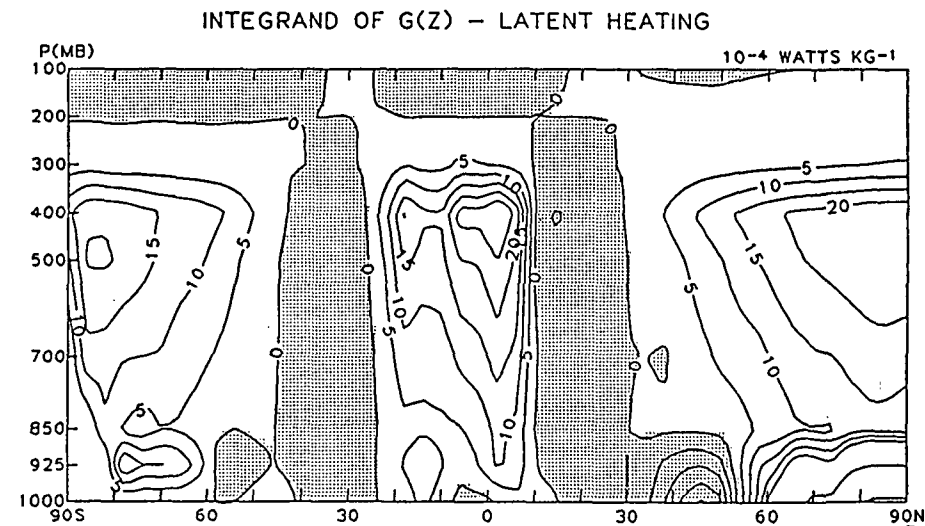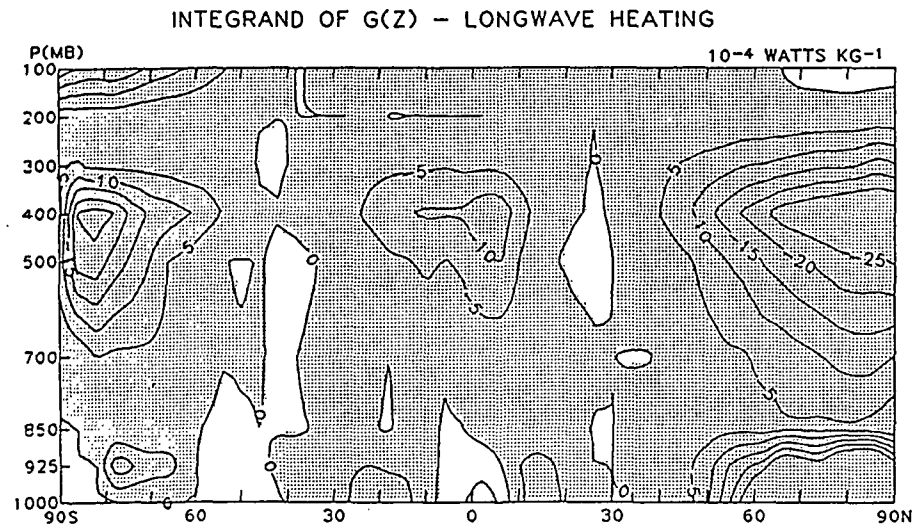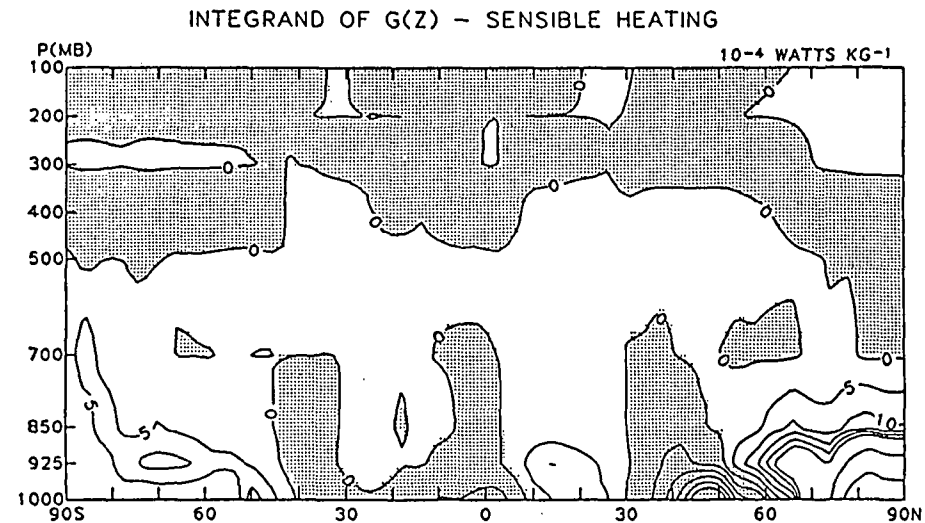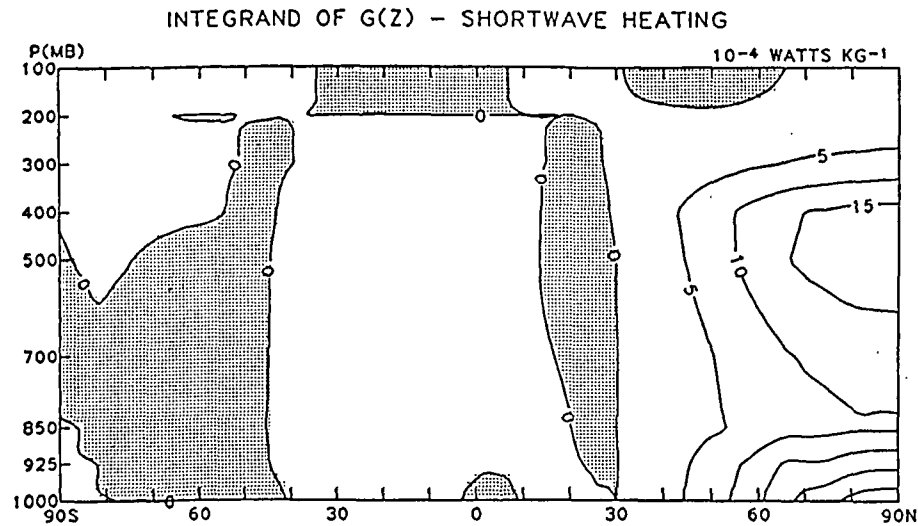
Fig. 5   Zonal mean integrand of the generation of zonal mean available potential energy by each of four heating components, for January 6 – February 4, 1979.

INTEGRAND OF G(Z) – DIABATIC HEATING

Fig. 6.   Zonal mean integrand of the generation of zonal mean available potential energy
by total diabatic heating, for January 6 – February 4, 1979.
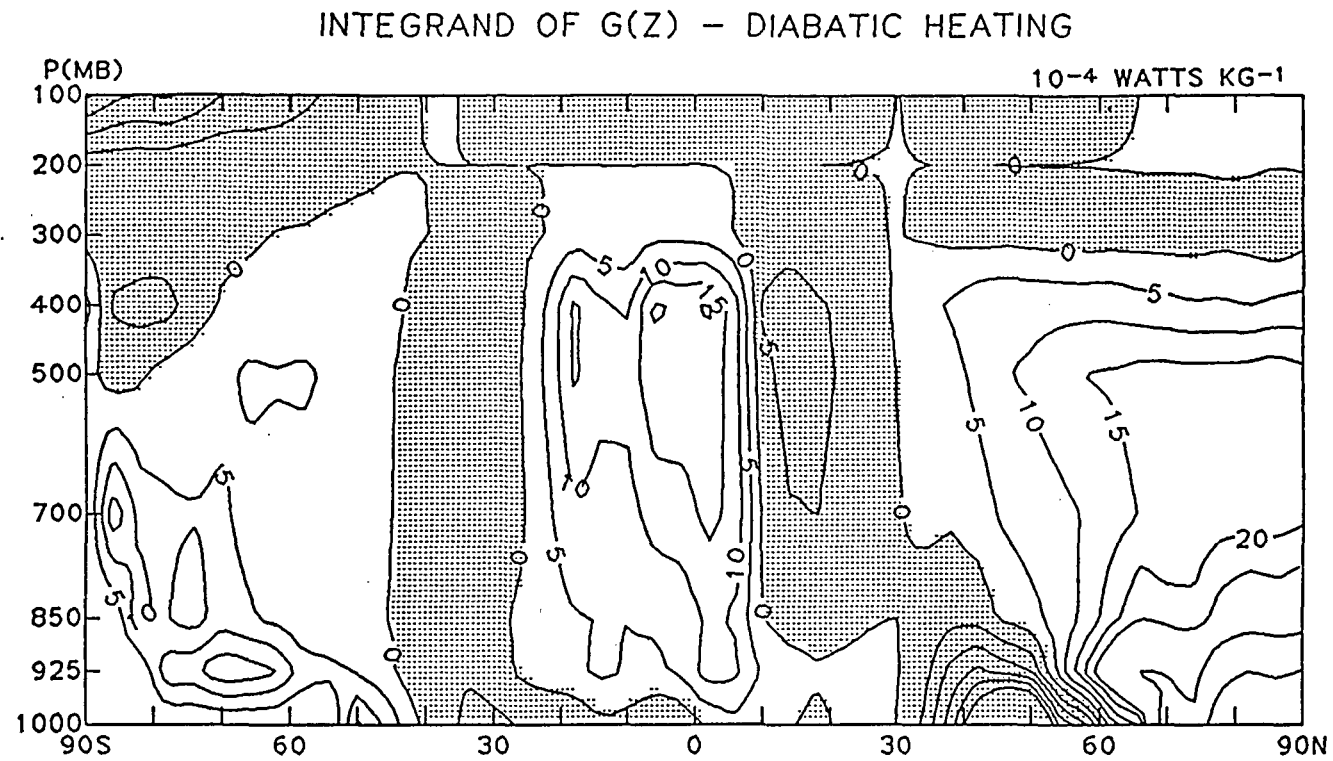
Fig. 7. Vertically integrated zonal mean integrand of the generation of zonal mean available potential energy by four heating components, for January 6 - February 4, 1979.

GENERATION OF ZONAL MEAN A.P.E.   WATTS M⁻²

TOTAL

Fig. 8   Vertically integrated zonal mean integrand of the generation of zonal mean available potential energy by total diabatic heating, for January 6 – February 4, 1979.

INTEGRAND OF G(E) — SHORTWAVE HEATING

P(MB)   10⁻⁴ WATTS KG⁻¹

INTEGRAND OF G(E) — SENSIBLE HEATING

P(MB)   10⁻⁴ WATTS KG⁻¹

INTEGRAND OF G(E) — LONGWAVE HEATING

P(MB)   10⁻⁴ WATTS KG⁻¹

INTEGRAND OF G(E) — LATENT HEATING

P(MB)   10⁻⁴ WATTS KG⁻¹

Fig. 9   Zonal mean integrand of the generation of eddy available potential energy by
each of four heating components, for January 6 – February 4, 1979. Isolines are
spaced at 2 x 10⁻⁴ W kg⁻¹.

INTEGRAND OF G(E) — DIABATIC HEATING
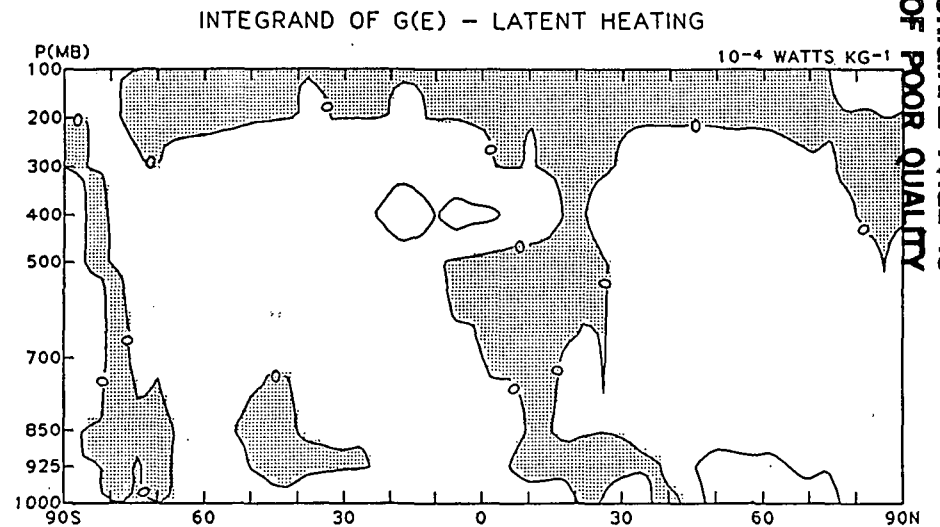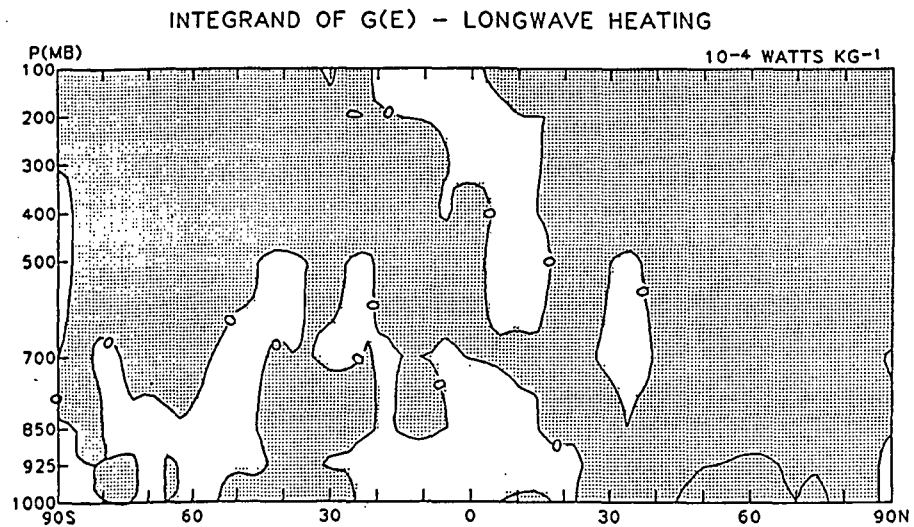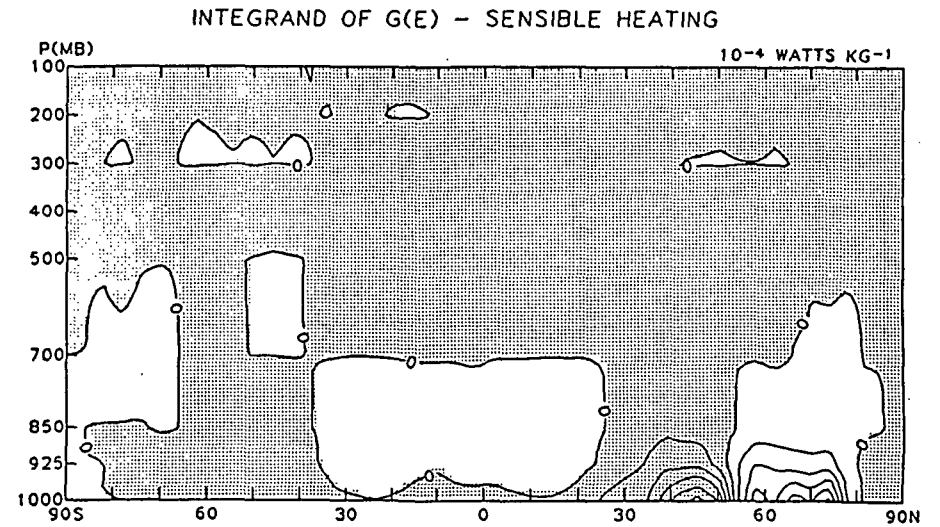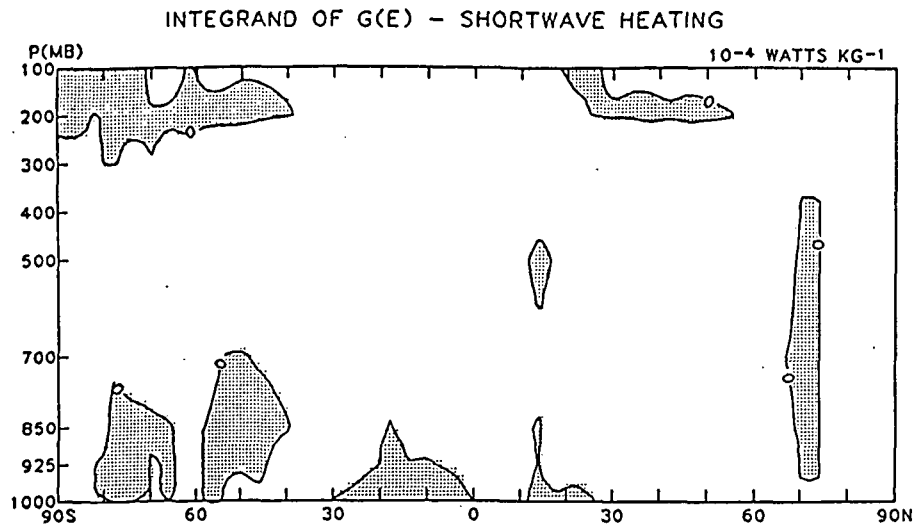
Fig. 10   Zonal mean integrand of the generation of eddy available potential energy by total diabatic heating, for January 6 – February 4, 1979. Isolines are spaced at 2×10^{-4} W kg^{-1}.
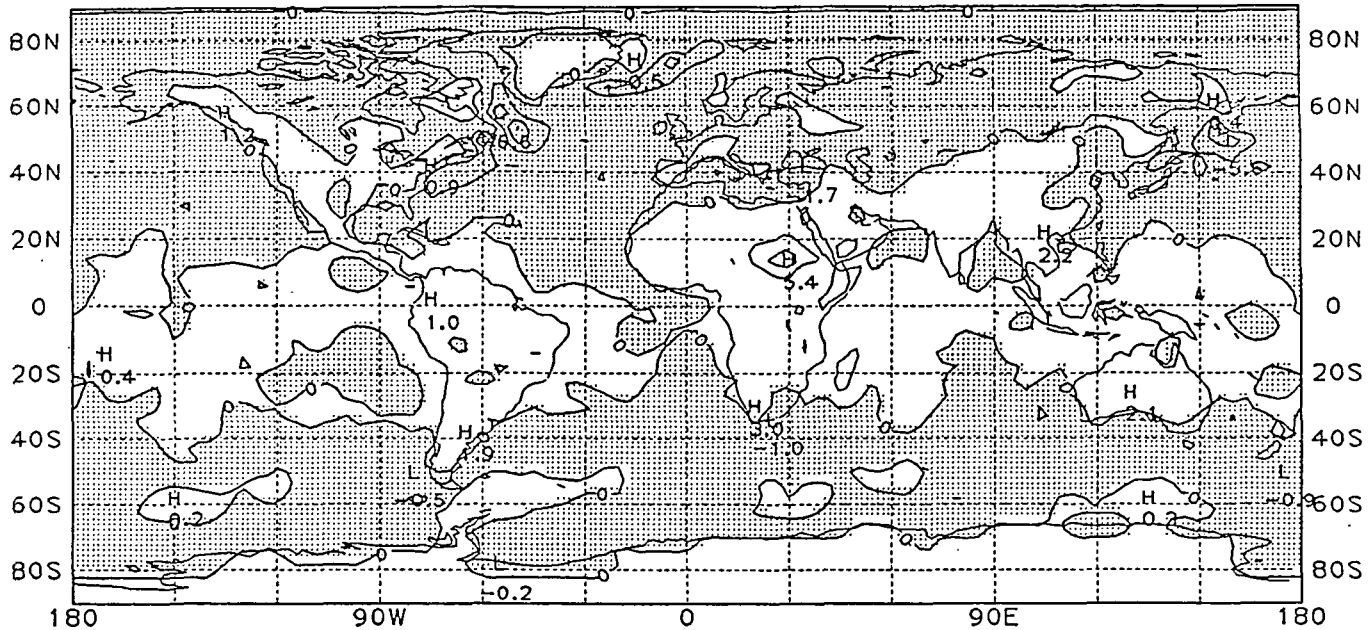
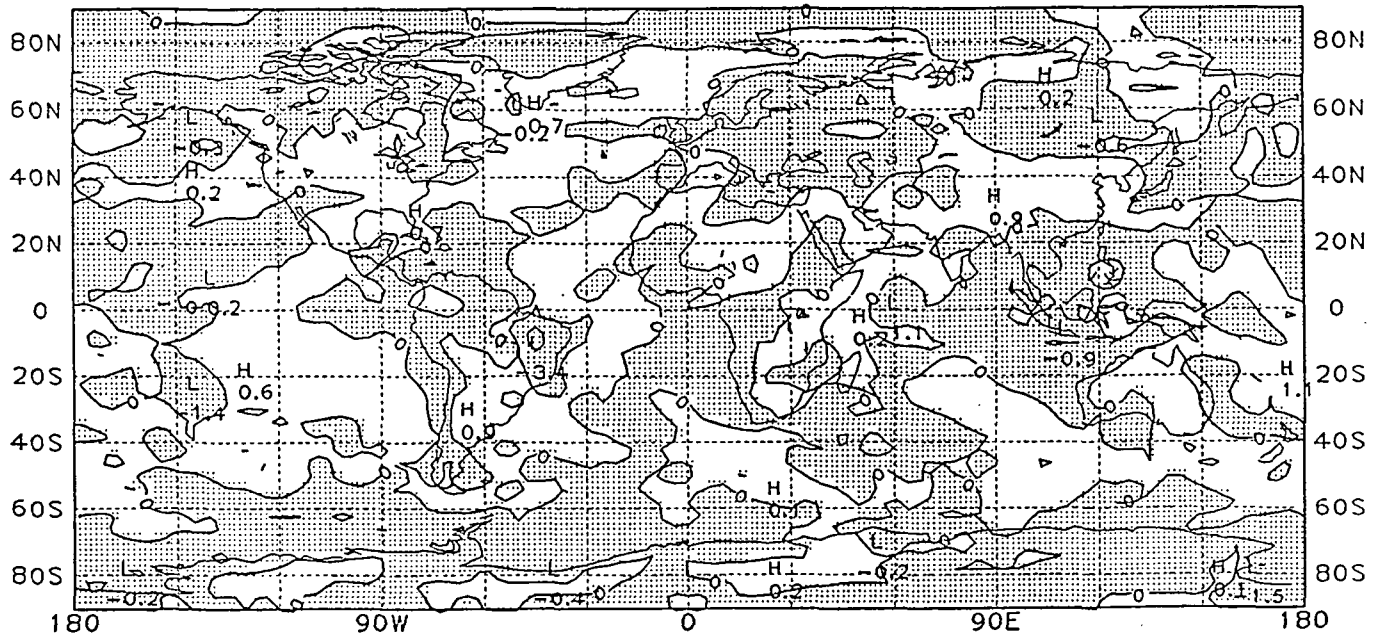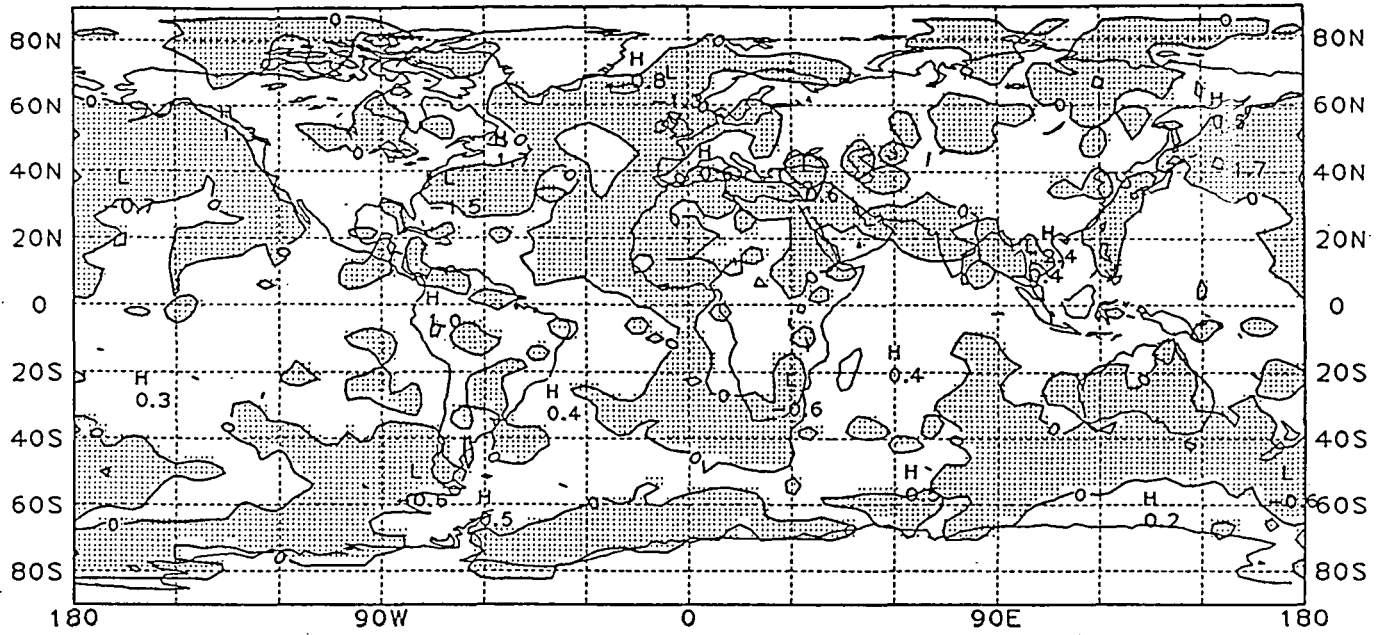CONTRIBUTION TO G(E) — TRANSIENT EDDY — DIABATIC HEATING   925MB
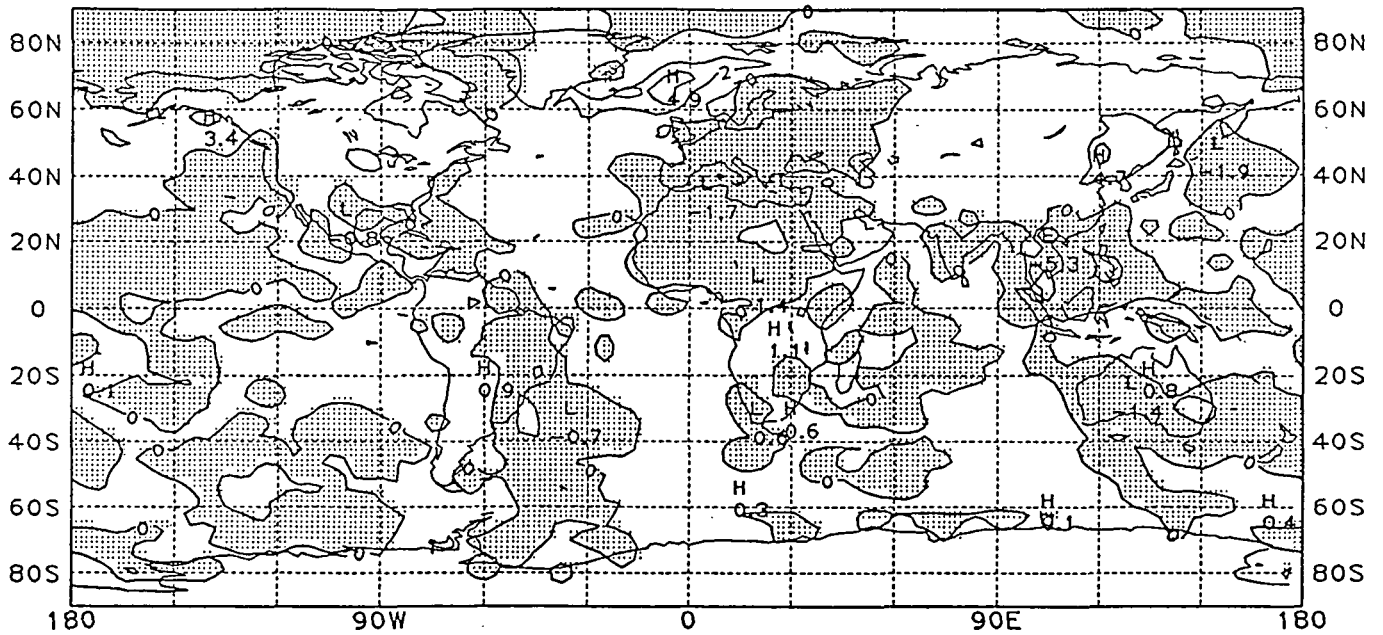

CONTRIBUTION TO G(E) — STANDING EDDY — DIABATIC HEATING   925MB

Fig. 11   Local integrand of the generation of transient and standing
eddy potential energy by total diabatic heating at the 925 mb
level for January 6 – February 4, 1979. Isolines are spaced
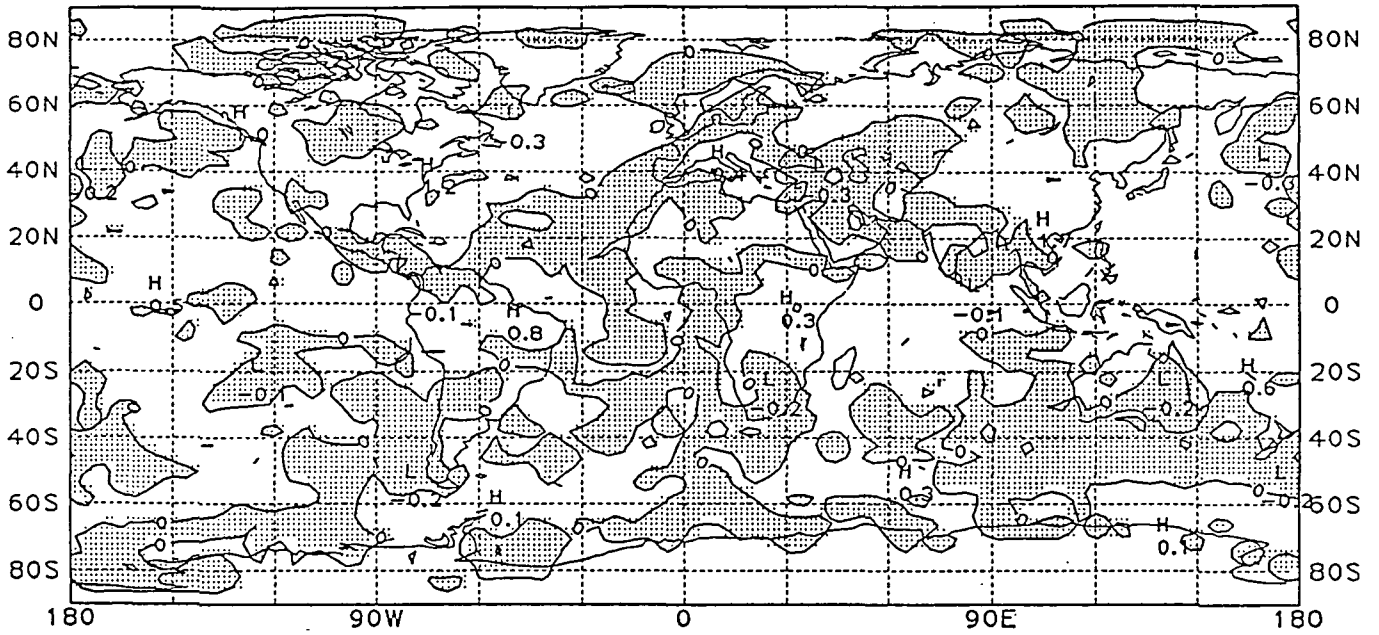at 2×10^{-4} W kg^{-1}.
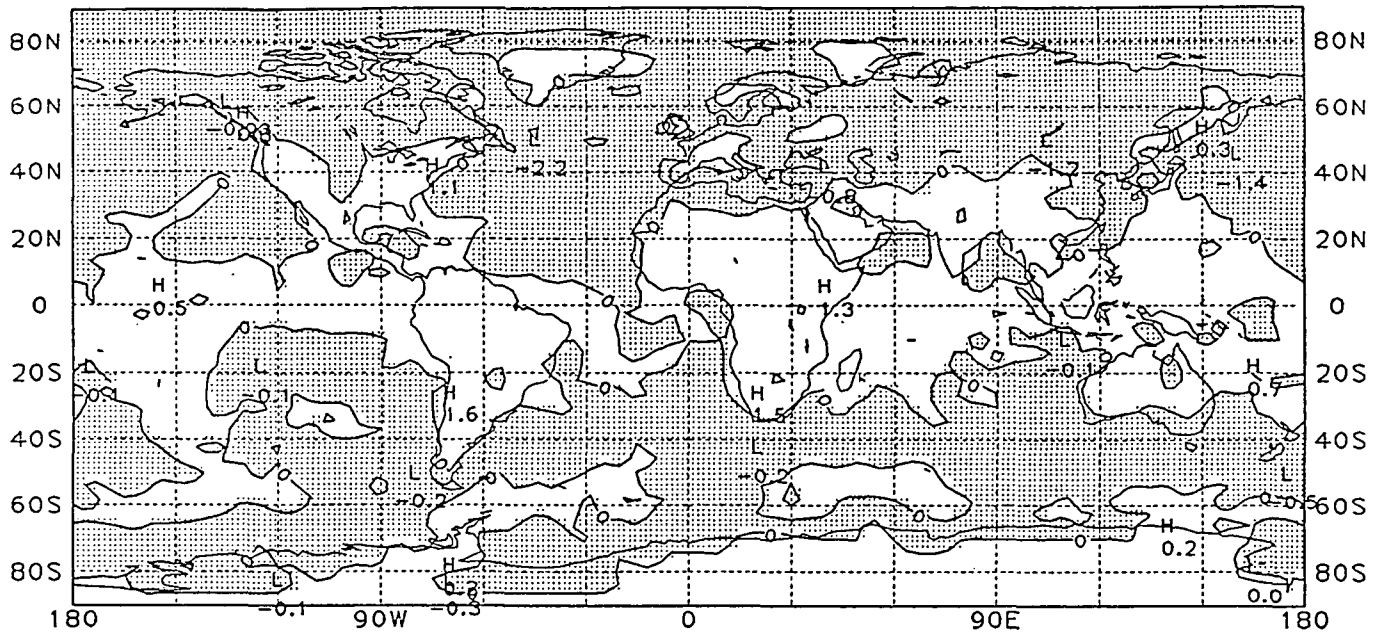
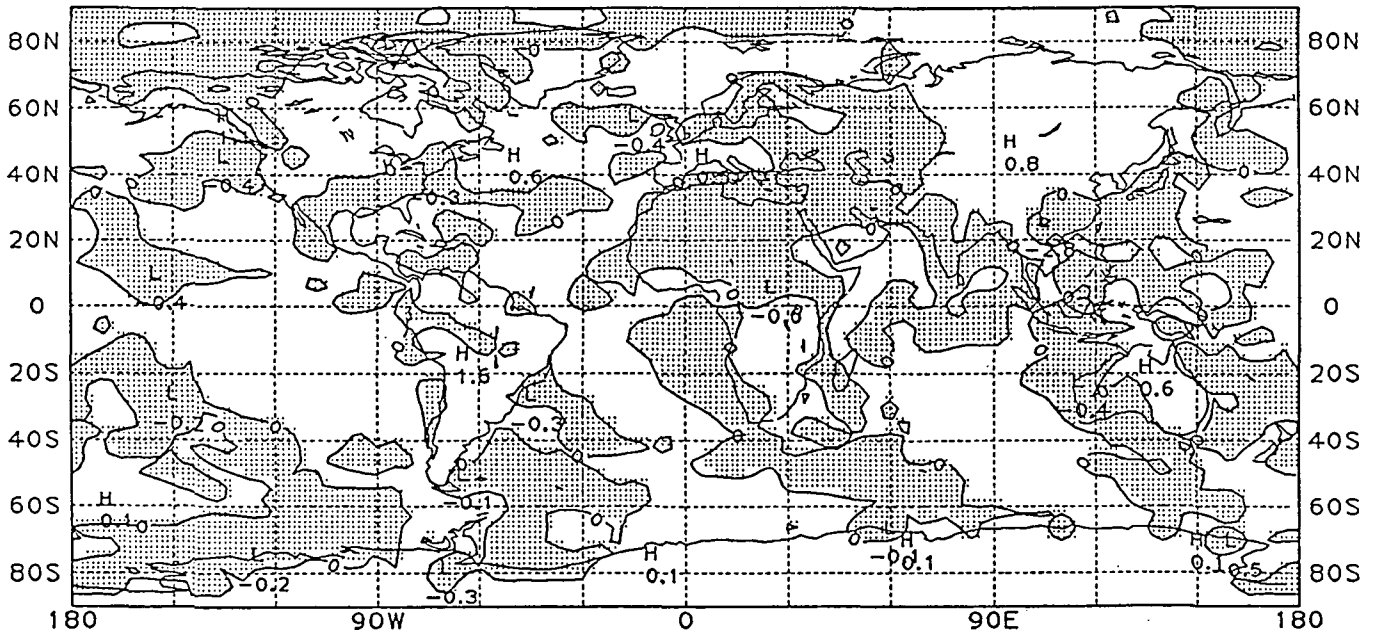CONTRIBUTION TO G(E) — TRANSIENT EDDY — DIABATIC HEATING   850MB
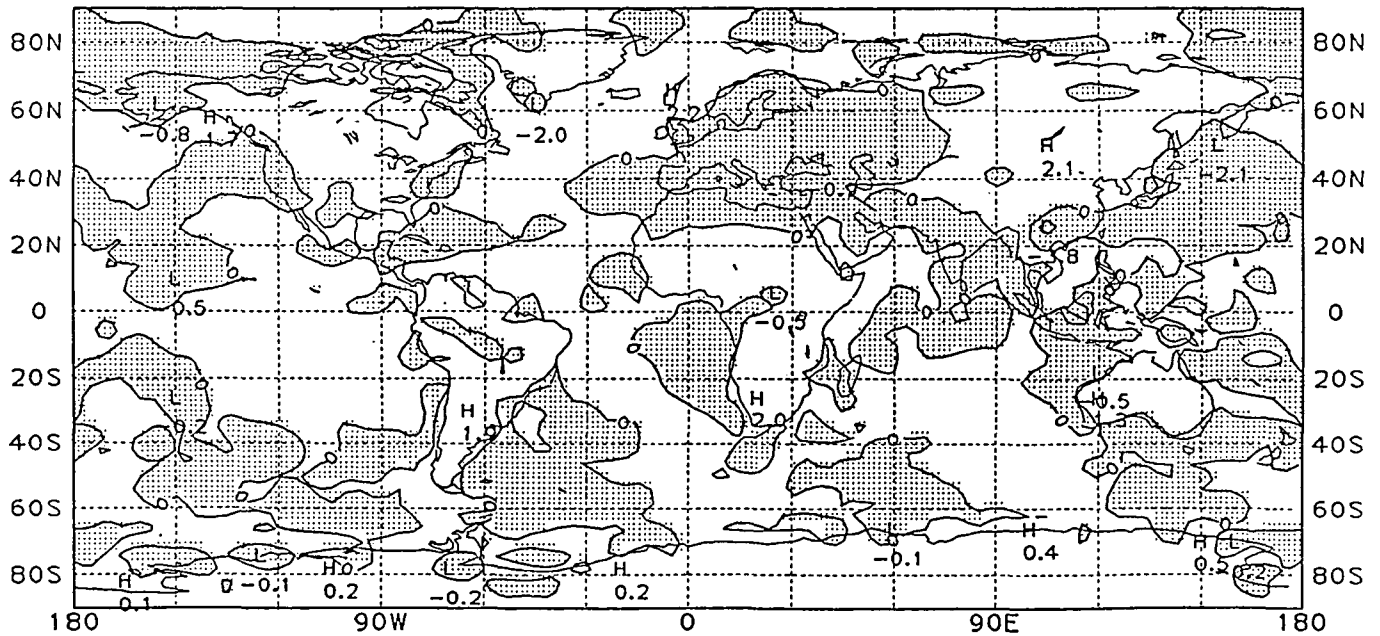
CONTRIBUTION TO G(E) — STANDING EDDY — DIABATIC HEATING   850MB

Fig. 12   Local integrand of the generation of transient and standing
eddy potential energy by total diabatic heating at the 850 mb
level for January 6 – February 4, 1979. Isolines are spaced
at 2×10^{-4} W kg^{-1}.
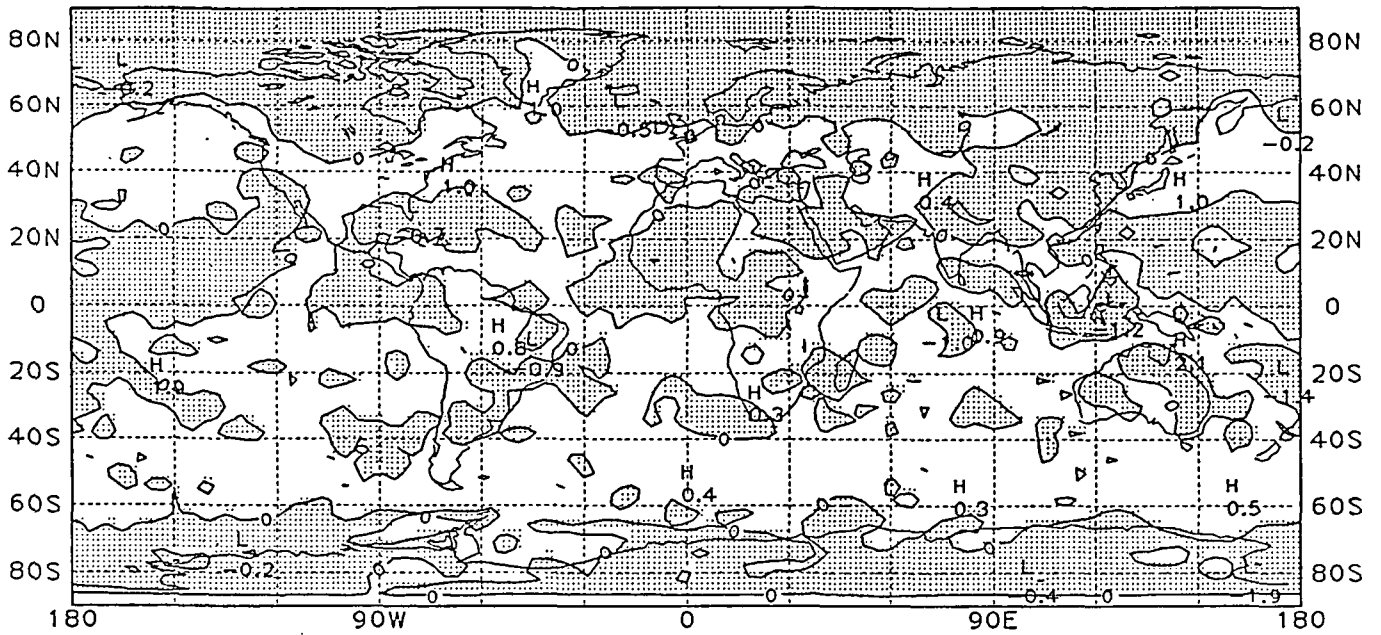
CONTRIBUTION TO G(E) — TRANSIENT EDDY — DIABATIC HEATING   500MB

CONTRIBUTION TO G(E) — STANDING EDDY — DIABATIC HEATING   500MB

Fig. 13   Local integrand of the generation of transient and standing
         eddy potential energy by total diabatic heating at the 500 mb
         level for January 6 – February 4, 1979. Isolines are spaced
         at 2×10^{-4} W kg^{-1}.

CONTRIBUTION TO G(E) — TRANSIENT EDDY — LATENT HEATING   925MB

CONTRIBUTION TO G(E) — STANDING EDDY — LATENT HEATING   925MB

Fig. 14   Local integrand of the generation of transient and standing eddy
           potential energy by latent heating at the 925 level, for January 6 —
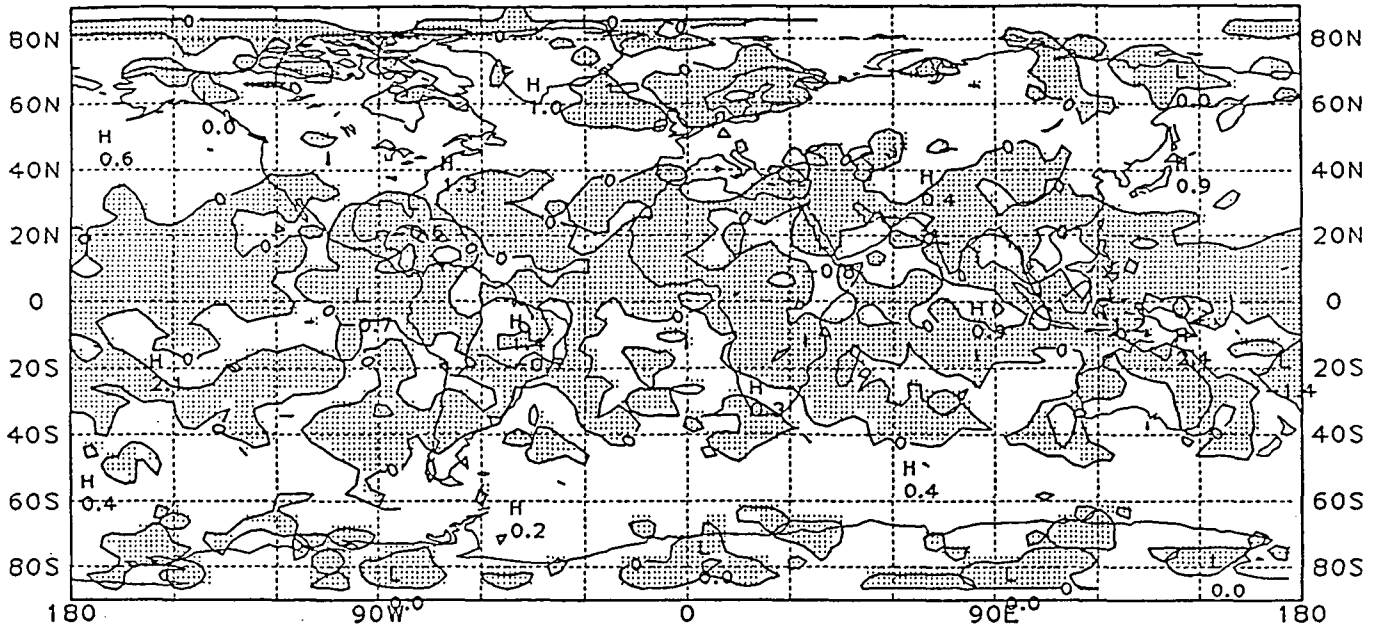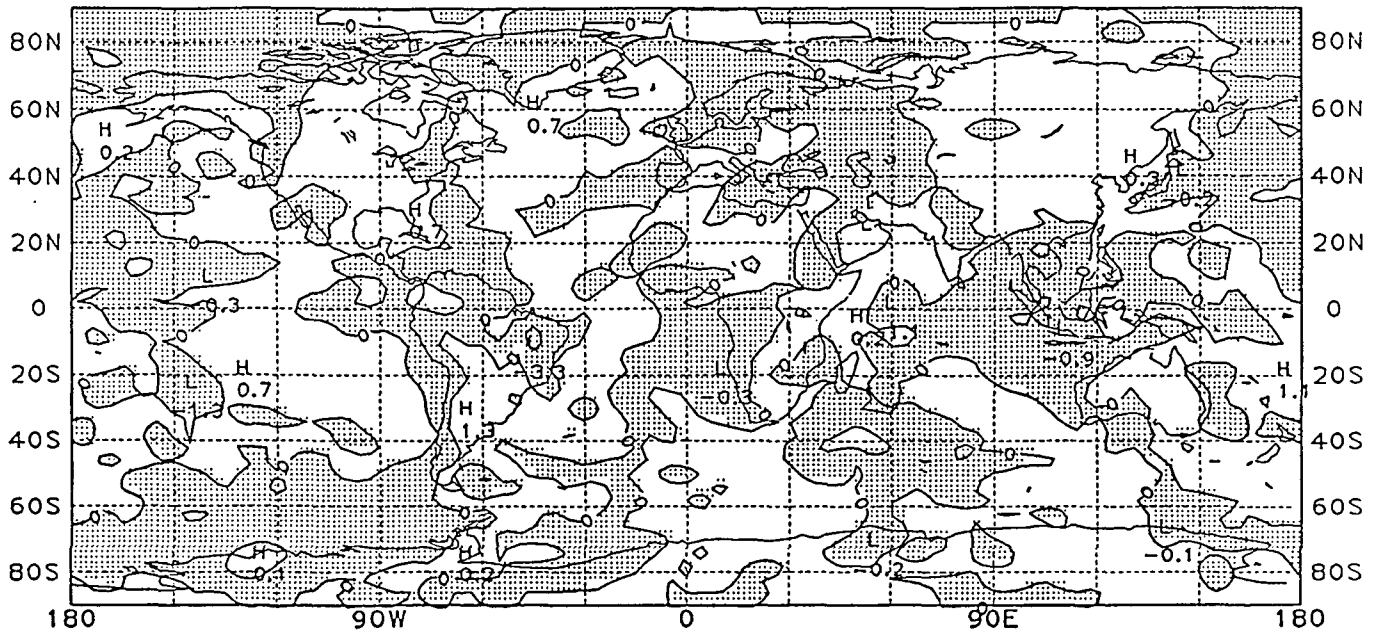   February 4, 1979.   Isolines are spaced at 2×10^{-4} W kg^{-1}.

CONTRIBUTION TO G(E) — TRANSIENT EDDY — LATENT HEATING   850MB

CONTRIBUTION TO G(E) — STANDING EDDY — LATENT HEATING   850MB

Fig. 15   Local integrand of the generation of transient and standing eddy
potential energy by latent heating at the 850 level, for January 6 –
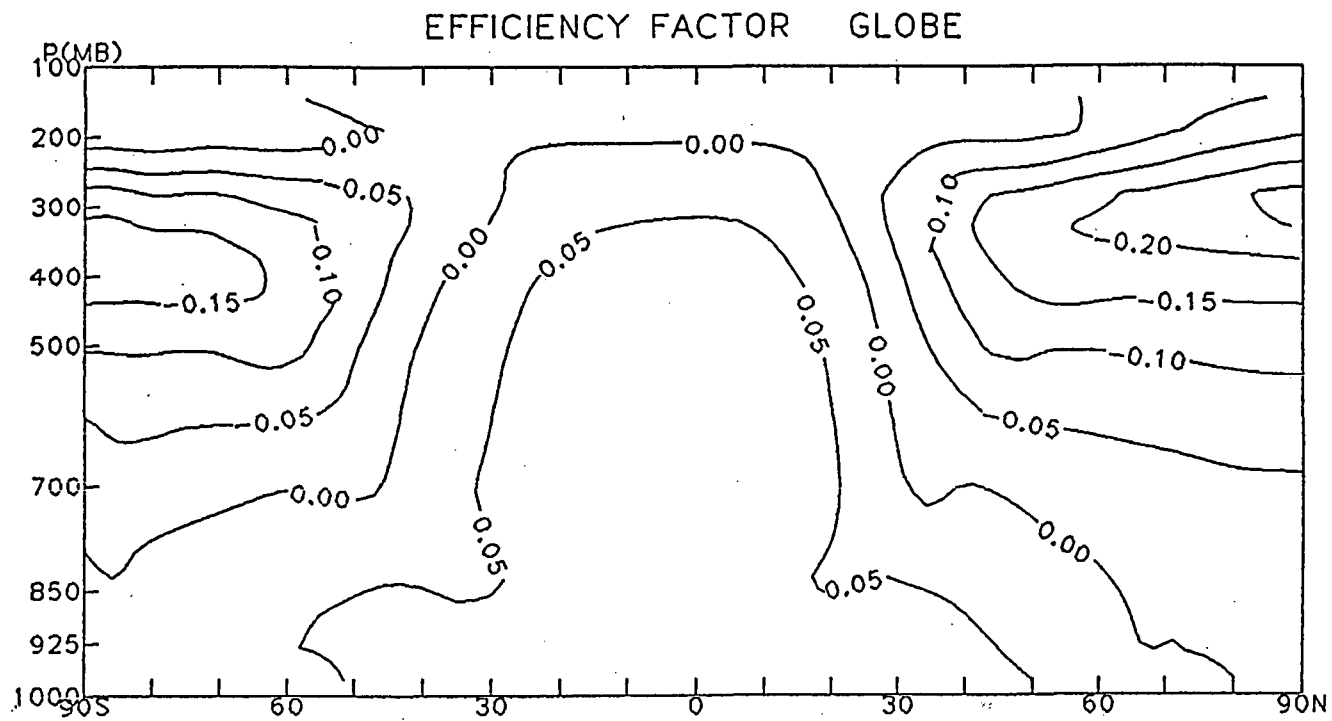February 4, 1979. Isolines are spaced at 2×10^{-4} W kg^{-1}.

CONTRIBUTION TO G(E) — TRANSIENT EDDY — LATENT HEATING   500MB

CONTRIBUTION TO G(E) — STANDING EDDY — LATENT HEATING   500MB

Fig. 16   Local integrand of the generation of transient and standing eddy
potential energy by latent heating at the 500 level, for January 6 –
February 4, 1979. Isolines are spaced at 2×10^{-4} W kg^{-1}.

Fig. 17   Efficiency factor, $[\overline{N}]$, for global generation of zonal mean available potential energy for January 6 – February 4, 1979.

GENERATION OF STANDING EDDY A.P.E. BY WAVENUMBER
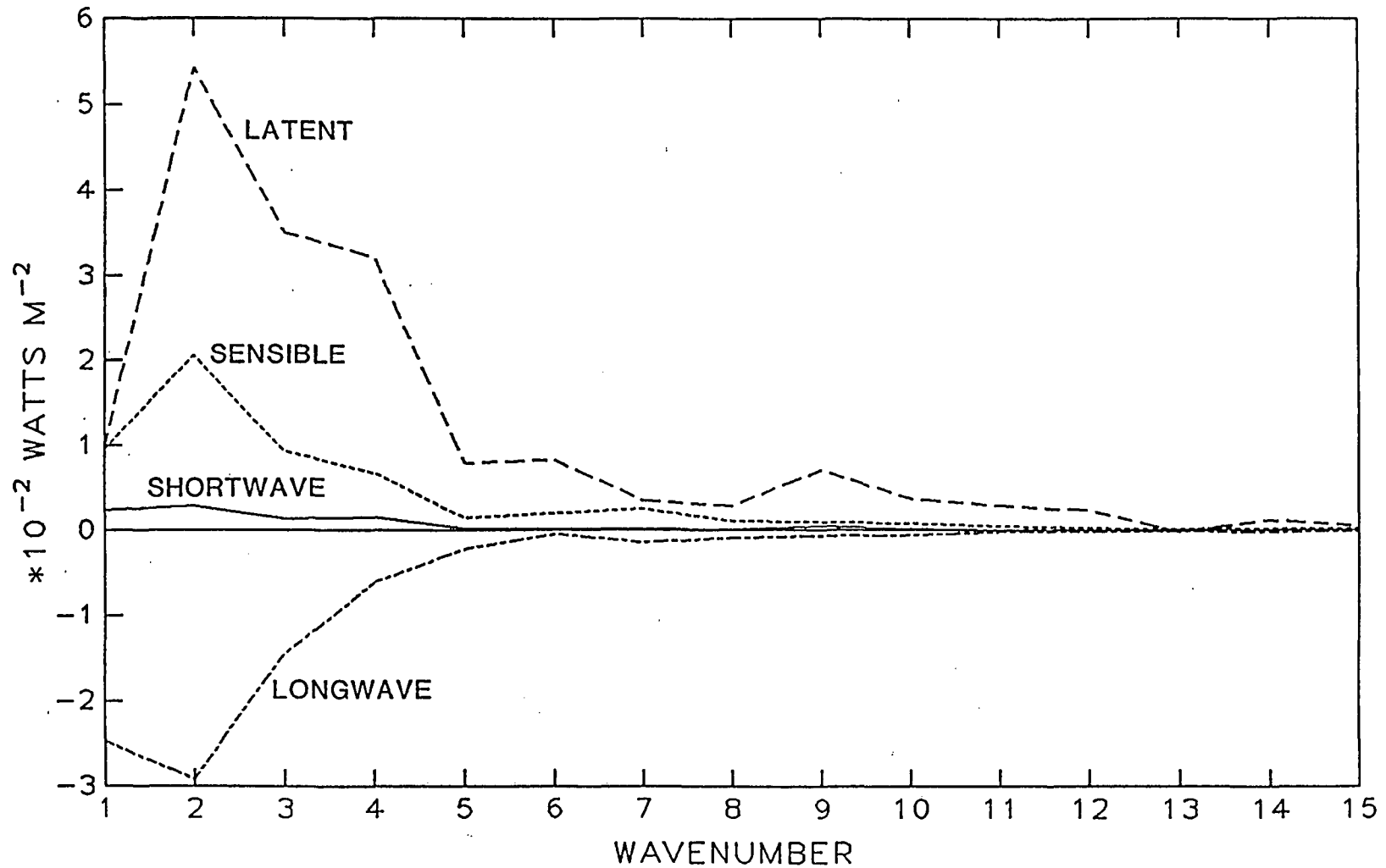
COMPONENTS

Fig. 18   Generation of standing eddy available potential energy for 15 longitudinal wavenumbers by each of four heating components, for January 6 – February 4, 1979.

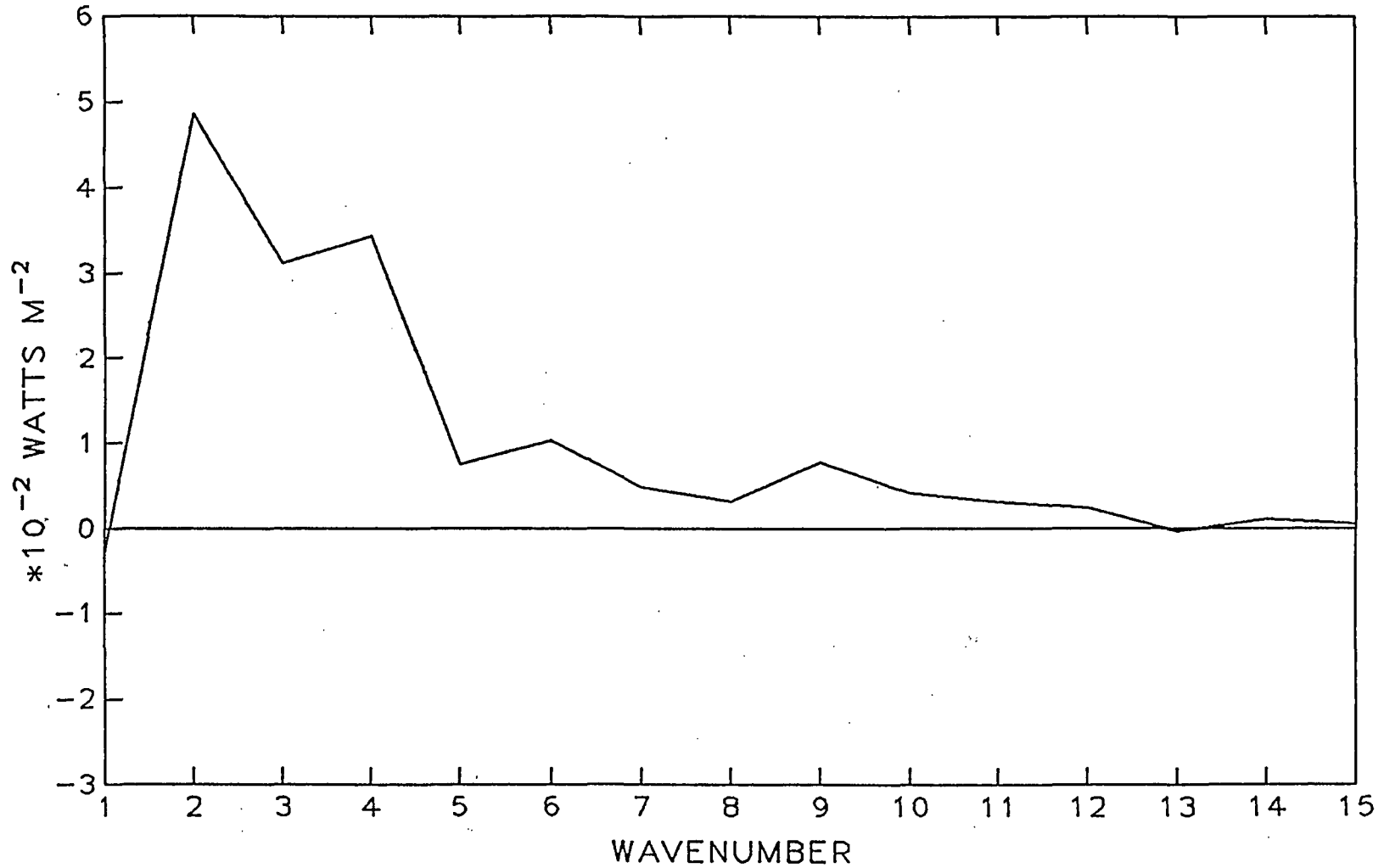# GENERATION OF STANDING EDDY A.P.E. BY WAVENUMBER

TOTAL

Fig. 19 Generation of standing eddy available potential energy for 15 longitudinal wavenumbers by total diabatic heating, for January 6 – February 4, 1979.
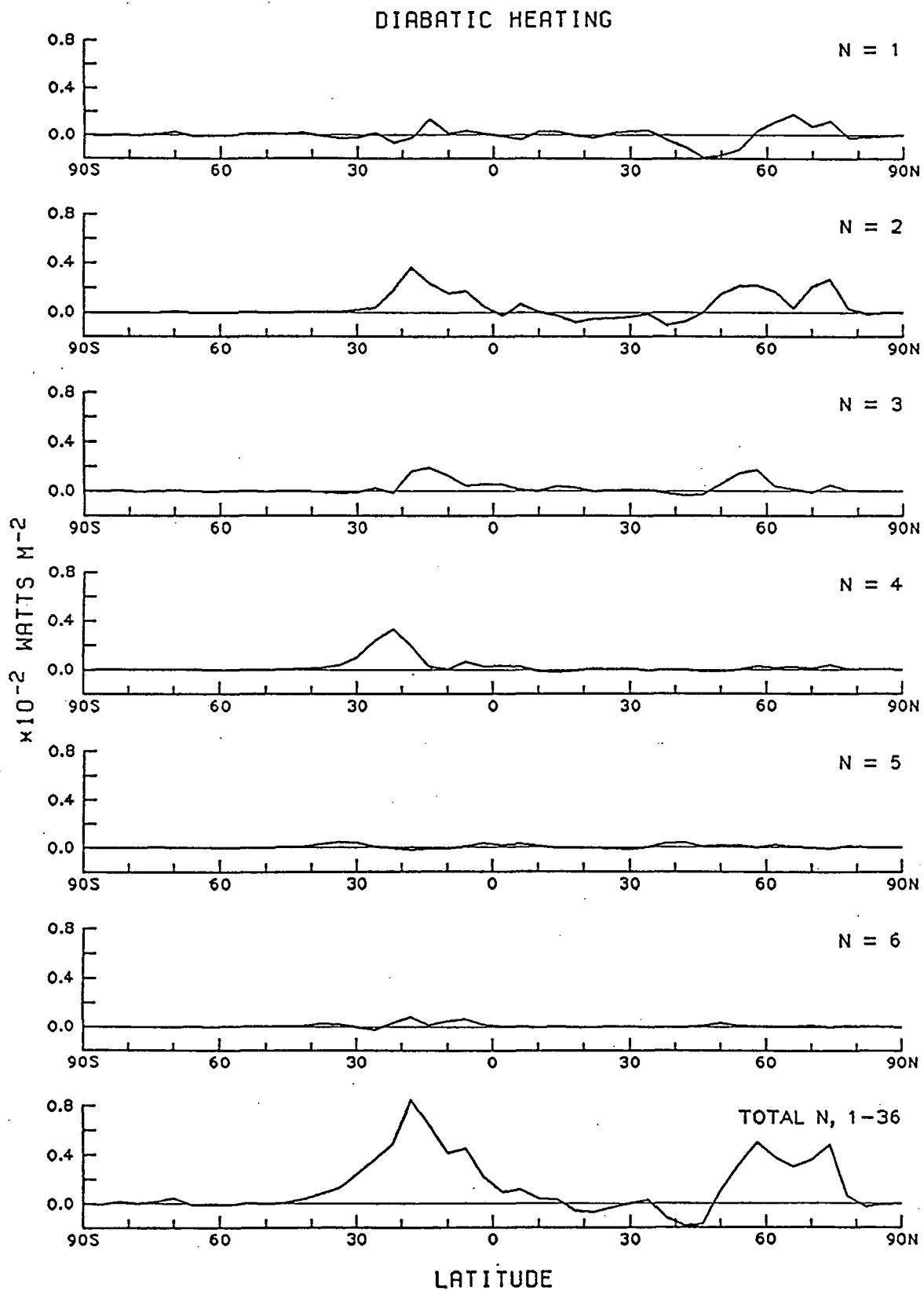
Fig. 20   Latitudinal distribution of the generation of standing eddy
available potential energy by wavenumber from total diabatic
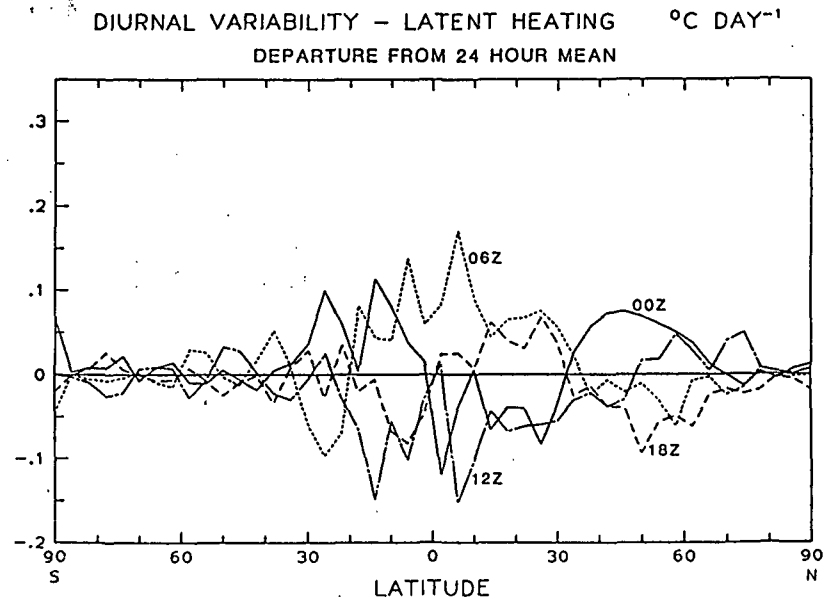heating, for January 6 – February 4, 1979.

DIURNAL VARIABILITY — SHORTWAVE HEATING   °C DAY⁻¹
DEPARTURE FROM 24 HOUR MEAN

DIURNAL VARIABILITY — SENSIBLE HEATING   °C DAY⁻¹
DEPARTURE FROM 24 HOUR MEAN

DIURNAL VARIABILITY — LONGWAVE HEATING   °C DAY⁻¹
DEPARTURE FROM 24 HOUR MEAN

DIURNAL VARIABILITY — LATENT HEATING   °C DAY⁻¹
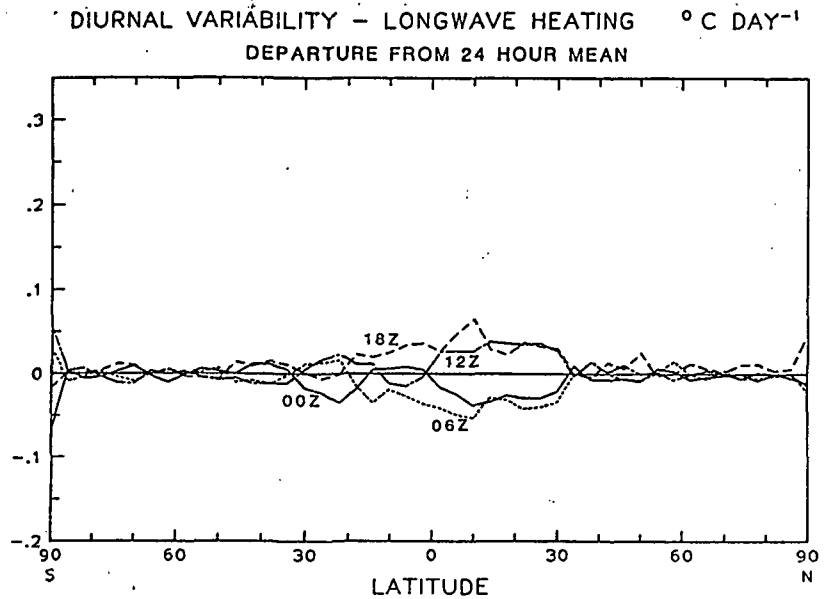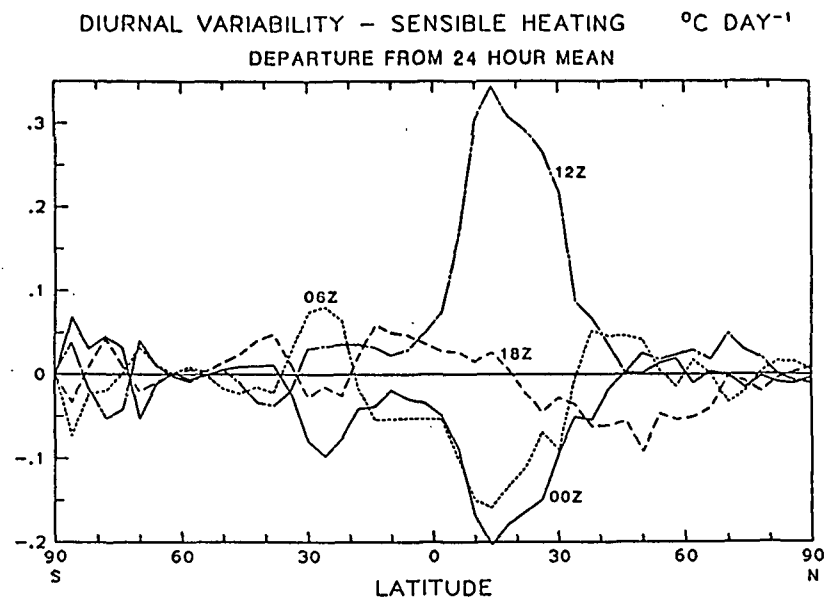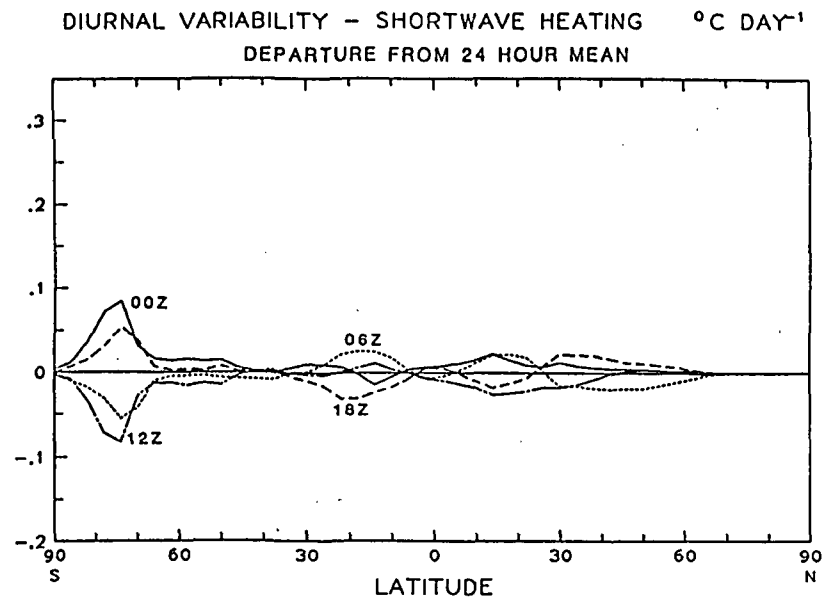DEPARTURE FROM 24 HOUR MEAN

Fig. 21   The departure from the 24-hour mean of zonal mean heating by each of four
heating components, for January 6 - February 4, 1979.